NANO LETTERS

2008
Vol. 8, No. 5
1314-1317

Probing Properties of Boron α-Tubes by *Ab Initio* Calculations

Abhishek K. Singh, Arta Sadrzadeh, and Boris I. Yakobson*

Department of Mechanical Engineering & Materials Science and Department of Chemistry, Rice University, Houston, Texas 77005

Received December 18, 2007; Revised Manuscript Received February 3, 2008

ABSTRACT

We investigate the properties of nanotubes obtained from recently described boron α-sheet, using density functional theory. Computations confirm their high stability and identify mechanical stiffness parameters. This allows one to further analyze the basic vibrations, including the radial breathing mode Raman frequency, $f_{RBM} = 210(\text{nm}/d)$ cm^{-1}. Careful relaxation reveals the curvature-induced buckling of certain atoms off the original plane. This distortion changes the overlap of the orbitals near the Fermi level and opens up the gap in narrow tubes, rendering them semiconducting. Wider tubes with the diameter $d \gtrsim 1.7$ nm retain original metallic character of the α-sheet. This combination of properties could make boron α-tubes (BT) an important material for electronic, bio- and chemical sensing, and optical applications.

Boron clusters of different shapes,[1–5] including nanometer-wide tubes,[5–11] have attracted attention of researchers for some years. Most recently, two theoretical observations have stimulated further focused interest to the field. One was the finding that boron can form rather stable hollow *spheres* similar to the well-known carbon fullerenes, including B_{65}, B_{92}, B_{110}, and particularly the boron buckyball B_{80}.[12] Another important observation was that, among the different possible 2D-planar assemblies of boron atoms, one particular pattern called the α-sheet[13,14] ensures the best occupancy of the bands by electrons and therefore has the lowest total energy. In different ways, both B_{80} and the α-sheet can be viewed as precursors for the boron tubes (BT) and suggest specific structure of the nanotube wall which previously remained a subject of debate.[5,8,11,15] Indeed, B_{80} can be "stretched" into a tube by a sequence of insertions of the equatorial rings,[16,17] as was often discussed in establishing connection between the carbon fullerenes and nanotubes. In this case a hemisphere of B_{80} or a larger fullerene naturally serves as possible closure cap to the tube (Figure 1a−c). Unfolding such uncapped cylinder yields exactly the α-sheet pattern, with the boron atoms missing at the right sites of the triangular lattice (Figure 1c→d). Inversely, one can start from the α-sheet as common precursor and wrap it into a fullerene sphere, with the 12 appropriate 60° wedge cutouts creating the pentagonal disclinations (Figure 1d→a). Yet more straightforward, the sheet[13,14] can be folded into a boron tube of a desired chiral twist and diameter (Figure 1d→c). One should point out that such "precursors" considerations are instructive from a theoretical point of view but have little to do with possible synthetic routes. Demonstrated preferred stability of the α-sheet[13] suggests that the tube obtained by wrapping its strip and reconnecting the covalent bonds should also be more stable than others, with the binding energy just slightly less than the sheet, due to the elastic strain of curvature. At the same time, electronic structure of such α-tubes originating from the metallic sheet is expected to remain metallic[13,14] (previously discussed other BT are also believed to be metallic[6,11,15]) irrespective of diameter and chirality, as opposed to carbon nanotubes (CNT), which could be both metallic and semiconducting.[18] Such unvarying metallicity, if confirmed, could be a great benefit compared

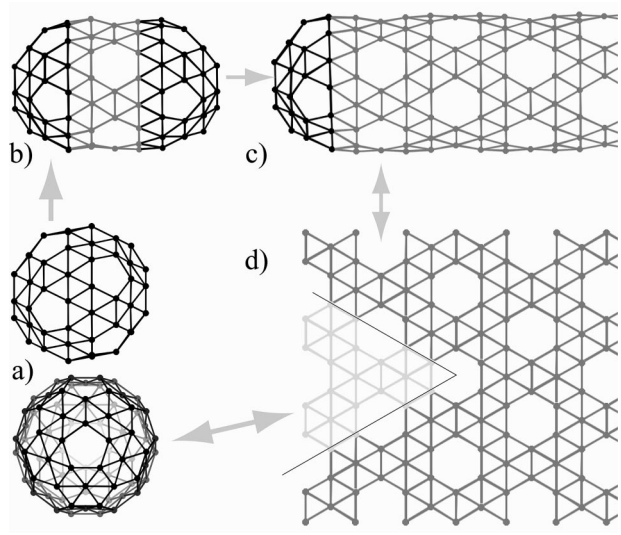

Figure 1. Schematics of interrelation between the B_{80} (a), which can be extended into prolonged cages like B_{120} (b) and further to nanotubes (c) by sequential insertion of the additional rings.[16,17] The tube in turn can be unfolded into α-sheet[13] (d). The shaded area in (d) marks the cut out for pentagonal disclinations when folding a sheet into B_{80} sphere.

* Corresponding author. E-mail: biy@rice.edu.

10.1021/nl073295o CCC: $40.75
Published on Web 04/01/2008

to the mixed types of the hard to separate CNT (separation remains a challenging task, which plagues the applications). Therefore, the prospect of having only metallic BT is considered as great advantage over CNT.[6–8,15] On the other hand, a lack of semiconductors among the BT could limit their applications in electronics, sensing, opto-electronics, etc.

Here we use *ab initio* calculations to verify that the boron α-tubes are stable, with the binding energy very close to that of the sheets. We further assess their mechanical stability in response to small deformations, calculate the basic stiffness constants, and find them to be comparable to the well-studied and somewhat stronger CNT and BNT[19–24] (boron−nitride tubes). On the basis of this, the radial breathing mode frequency, detectable by Raman spectroscopy and often used as a signature for hollow tubes, can be computed for arbitrary α-tubes. In spite of their overall stability, we observe that the cylindrical curvature causes a degree of buckling, with specific boron atoms departing from their in-plane positions. This buckling appears to have profound effect on the electronic structure. The tubes with the smaller diameters are semiconducting, while for $d \gtrsim 1.7$ nm they retain metallic no-gap band structure of the α-sheet ($d = \infty$).

The structural optimization for a set of nanotubes below is performed using density functional theory incorporating electron and ionic core interactions with the projected augmented wave method with a plane wave basis set employing periodic boundary conditions and the conjugate gradient technique within the generalized gradient approximation (GGA) of PBE[25] for the exchange-correlation energy.[26–29] The cutoff energy for the plane wave expansion is taken to be 318 eV. The one-dimensional Brillouin zones of different nanotubes are sampled by equivalent set of *k*-points, which are also sufficient to converge the energies. The structures are considered to be fully relaxed when the absolute value of the force on each ion becomes less than 0.001 eV/Å; this strict criterion is important not to miss structural details such as atomic buckling. No less than 14 Å vacuum space is used in lateral directions to avoid any interactions between the periodic images of the nanotubes.

Table 1. Calculated Stiffness (C), Poission Ratio (ν), and Radial Breathing Mode Frequencies (f_{RBM}) of Boron α-Tubes

nanotubes	diameter (Å)	C (N/m)	ν	f_{RBM} (cm^{-1})
(5,5)	8.13	209.4	0.18	238.9
(9,0)	8.63	206.7	0.21	224.8
(6,6)	9.93	202.1	0.26	195.9
(12,0)	11.31	204.6	0.21	170.6
(7,7)	11.37	215.2	0.20	173.7
(8,8)	13.13	214.0	0.21	150.2
(18,0)	16.50	217.5	0.15	119.2

Calculating the α-sheet with the above-described method yields the binding energy ($E_b = 5.99$ eV) and bond length ($b = 1.67$ Å) close to the values of Tang et al.[13]

For naming purposes, we choose the indexing of the BT to correspond to the long-accepted convention for the CNT and BNT: with the two $\sqrt{3}b$-long basis vectors 60° apart, each directed along the zigzag motif in the lattice, the tube circumference is specified as a pair of components (n,m). This implies that any (n,m) tube derived from α-sheet exists only when ($n - m$) is a multiple of three. The diameter of the (n,m) tubes can be given by the formula $d = 0.94(n^2 + m^2 + nm)^{1/2}$ Å. In order to explore the mechanical and electronic properties of the α-BT somewhat comprehensively, we consider both armchair and zigzag types (Table 1). We choose three zigzag BT to cover a reasonable range of diameters which can reveal the common physics, with indexes (9,0), (12,0), and (18,0). For the armchair BT, we study four nanotubes with varying indexes and diameters, (5,5), (6,6), (7,7), and (8,8). We find that relaxation is very much diameter dependent and occurs mostly around the filled hexagons, where the central boron atom B_c is inserted, relative to a hexagon tiling of graphene type. Generally, these central B_c atoms buckle inward by departing off the plane of the hexagons (Figure 2c, inset). Not all the central B_c atoms buckle, but this rather happens in every other filled hexagon. With the increasing diameter, the central atoms B_c systematically move back into plane of the hexagons (Figure 2c). This mode of geometrical relaxation appears to have important effect on the electronic structure of the nanotubes, as discussed later.

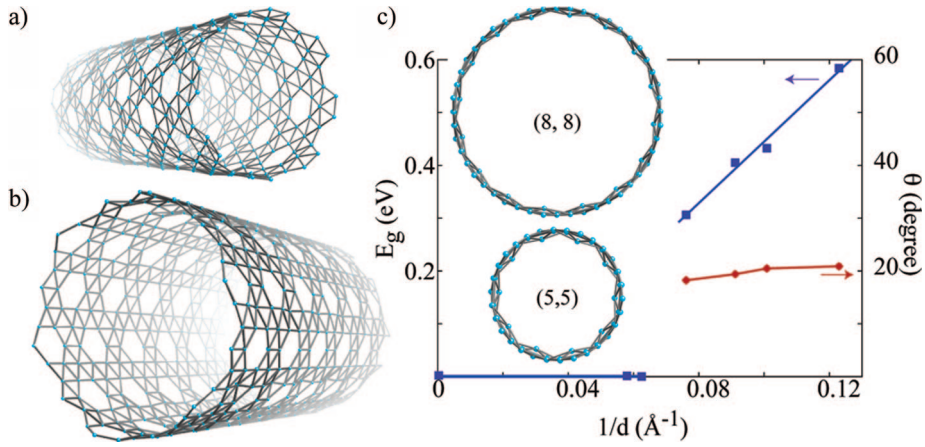

Figure 2. Relaxed structure of (a) armchair (8,8), and (b) zigzag (18,0) α-tubes. Part (c) shows plots of the band gap E_g (left axis) and dihedral angle θ formed by the B_c atom and the plane of hexagon (right axis) vs curvature, 1/d, for the studied armchair nanotubes. Axial view of (5,5) and (8,8) α-tubes illustrates the degree of atomic buckling, inset in (c).

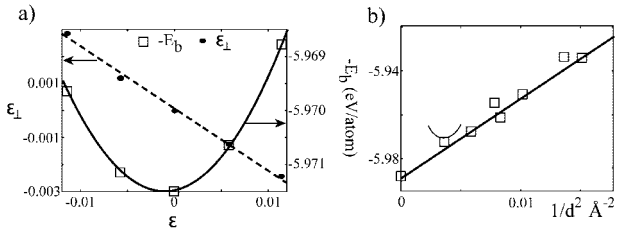

Figure 3. (a) Square parabola of the energy per atom with the axial strain ε, here for (8,8) tube, is used to compute the wall in-plane stiffness C for the α-tubes. The straight line shows the radial reduction $\varepsilon_\perp$ vs tensile strain ε, to yield the Poisson ratio, ν. (b) Plot of $E_b(d)$ vs square of the inverse diameter of BT. The intercept of this curve with y-axis gives the binding energy for the α-sheet, which agrees well with directly computed $E_b(\infty) = 5.99$ eV/atom.

In order to be practically realizable and possibly useful in applications, the nanotubes should be able to stand some mechanical deformations. We evaluate the mechanical stiffness of the BT by calculating the in-plane stiffness C, the Poission ratio ν, and the flexural rigidity D of their wall. (The hexagonal symmetry of two-dimensional lattice of α-sheet ensures its isotropic elastic properties and thus allows one to replace the atomistic structure by the continuum shell model with appropriate parameters.[30]) Computing the energy E per atom as a function of elongation ε under uniaxial tension yields the value of $C = (1/a)(\partial^2 E/\partial\varepsilon^2)$, where a is the area per atom in the α-sheet. The Poisson ratio ν can be evaluated from the ratio of relative reduction of the diameter $\varepsilon_\perp$ and the axial strain ε. Figure 3a shows one such example of calculation of C for (8,8) armchair BT, where energy per atom as a function of elongation strain ε is plotted and fitted to a parabola, $\sim{}^1/_2 C\varepsilon^2$. We also show within the same graph the change of diameter with the elongation, which gives us the Poisson ratio. The values for C and ν for all considered BT are given in Table 1. The overall variation in the values of C is within 8% of an approximate value $C = 210$ N/m. The values of ν around 0.2 show a similar variation.

In addition to in-plane stiffness C, the value of flexural rigidity D can be defined as a coefficient in the energy of unloaded/free relaxed tubule as a function of its diameter d, $E_b = \text{const} + 2D/d^2$, where E_b is the equilibrium binding energy/atom of the tubule. The flexural rigidity gives the dependence of the energy on the curvature of a 2D sheet. Since both zigzag and armchair BT are formed by wrapping of the same α-sheet, this value should be similar for both. In Figure 3b we plot the E_b as a function of curvature, and the data fit well to a straight line whose intercept with y-axis gives the $E_b = 5.99$ eV/atom of the α-sheet. The half of the slope of this line gives the value of $D = 1.82$ eV Å^2. Thus the resistance to mechanical deformation for BT is quite high (within 60% of CNT parameters[19,22]). Knowledge of C and D constants permits to rather fully characterize the elastic mechanical behavior of the BT. For example, another important measure of stiffness is so-called persistence length[31] l_p (a correlation length for the direction of a tube exposed to equilibrium fluctuations at temperature T). Its magnitude is proportional to the tube stiffness, $l_p = \pi C d^3/8k_bT$, and amounts to fraction of a millimeter at room temperature for the typical nanometer diameters. Such structures would not only be able to sustain some incidental strain but also may be used for some mechanical applications.

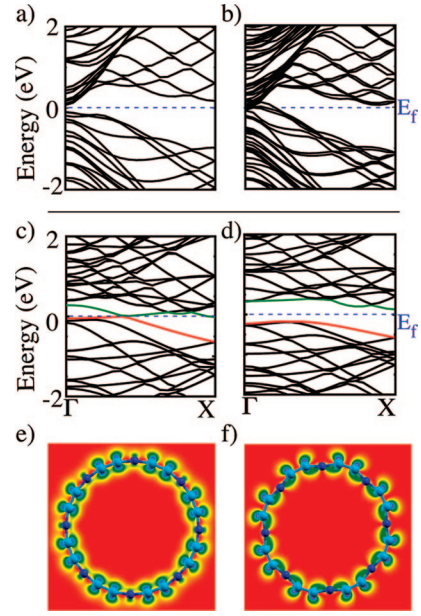

Figure 4. Band structure of (a) zigzag (18,0), (b) (21,0), (c) unrelaxed, and (d) relaxed armchair (8,8) tubes. Band-decomposed charge density in the plane perpendicular to the axis, for the highest occupied bands (e) for unrelaxed and (f) for relaxed (8,8) tube. The dark blue atoms are the central B_c atoms, which buckle upon the relaxation.

Furthermore, knowledge of the shell parameters allows one to calculate some vibrational frequencies without embarking into full analysis of all molecular vibration modes. Of particular interest for identification of hollow structures is the radial breathing mode (RBM) frequency f_{RBM}.[32] It can be easily obtained as $f_{RBM} = (1/\pi cd)/[(C/(1-\nu^2)\rho_s)^{1/2}]$, where ρ_s is the mass density of the sheet per unit area. (The speed of light c is to convert to spectroscopic cm^{-1} units.) The values for f_{RBM} are given in Table 1 and can be generally estimated as $f_{RBM} \approx 210$ nm/d, cm^{-1}. Extrapolating to the $d = 3$ nm yields the breathing mode frequency near 70 cm^{-1}. This differs from the breathing mode frequency detected in the Raman spectra,[7] which may indicate some underlying difference in the actual structures. (Note that the corresponding value for CNT is 76 cm^{-1}, based on well-established parameters for carbon.[19,32])

Turning to the electronic properties of these nanotubes, we find that all the zigzag and armchair nanotubes with smaller diameters are semiconducting (Figure 4a,d). While the sheet is originally metallic, in cylindrical BT large enough curvature and consequential buckling do open the gap. The gaps in armchair nanotubes are indirect and lie within the range of ~0.6 eV (Figure 2c). Indeed, one can analyze the origin of this unexpected gap opening by calculating the band structure of *unrelaxed* armchair BT. In this case, they remain metallic (Figure 4c). On the other hand, when fully *relaxed*, same nanotubes become semiconducting (Figure 4d). To further clarify the role of buckled B_c atoms, we have analyzed the band-decomposed charge densities of the valence band maximum (VBM) of relaxed and unrelaxed

(8,8) BT (example plotted in Figure 4e,f for VBM of unrelaxed and relaxed tubes). One can see that the charge density of the VBM originates from the buckled B_c atoms and their nearest neighbors. In Figure 4e,f, we can clearly see the effect of rehybridization on the B_c atoms induced by the buckling, in terms of the change in the contribution from those atoms to the electron density. Since this buckling does not break the symmetry of the nanotubes, opening of the gap should not be attributed to Jahn–Teller type of distortions but appears to be due to rehybridization. As the dihedral angle formed by the B_c atom and the plane of the hexagon decreases (Figure 2c), the nanotube eventually transforms into metal. (In an analogous way, small off-plane displacements of the B_c atoms in B_{80} result in several similar isomers, with possible ripple-transformations among them.[33]) We have explicitly verified this by performing calculations on few selected armchair and zigzag tubes with the larger diameter [e.g., (10,10), (11,11), (21,0), and (24,0)].

Owing to the metallic nature of α-sheet, this transition to metal is very much expected. The band structure of a (21,0) BT is shown in Figure 4b, where several bands visibly cross at the Γ-point. This is because Γ-point of the zigzag BT coincides with that of the sheet, unlike armchair BT. These bands are highly dispersive, implying that the effective mass of the charge carriers should be very small, leading to high mobility and better conductivity. There are several bands in the vicinity of the Fermi level, which also ensures the large carrier density. The metallicity of the larger diameter BT, low effective mass, high mobility, and conductivity qualify the BT as good conductors at nanoscale, and hence they could potentially be used as metallic interconnects in electronic devices.

In summary, we study the mechanical and electronic properties of pure boron nanotubes derived by wrapping the recently predicted as most stable α-sheet.[13] While stability of such α-tubes could be anticipated (being derived from a stable sheet), we do verify it by direct energy minimization. Calculations allow one to obtain the mechanical parameters of boron α-tubes such as stiffness $C \approx 210$ N/m, Poission ratio $\nu \approx 0.2$, and flexural rigidity $D \approx 1.8$ eV Å^2. We further show how the basic vibrational frequencies for the α-tubes can be calculated, with the Raman detectable radial breathing frequency as important example. We note that its computed value differs noticeably from the reported one based on Raman spectroscopy experiments.[7] The discrepancy may indicate that the actual BT have structure distinctly different from the α-tubes, or their stiffness in the sample is affected by additional lateral forces, and calls for future investigation of these structures. (In fact, one of the observed Raman peaks[7] is close to the RBM frequency of B_{80}, 420 cm^{-1}.) The α-tubes have a clear distinction in their electronic properties as the tubes of smaller diameters open the band gap and are semiconductors, according to our calculations. We relate the origin of semiconductor gap in BT to the specific relaxation buckling in atomic positions, which leads to rehybridization of the orbitals. While the obtained mechanical properties appear rather robust and uniform among the tubes, further studies are necessary to determine the broader range of electronic properties, to include the chiral tubes as well. Nevertheless, the combination of emerging features makes boron α-tubes (BT) promising material for electronic, bio- and chemical sensing, and optical applications.

Note Added in Proof: After the submission of our work, a report[34] appeared with the analysis of a boron sheet, apparently independent from ref 13, and also describing the electronic gap in the BT, in general agreement with the discussion above.

Acknowledgment. Work was supported by the Robert Welch Foundation (C-1590), the Office of Naval Research (program manager P. Schmidt), and the National Science Foundation (award 0708096).

References

(1) Zhai, H.-J.; Kiran, B.; Li, J. L.; Wang, L.-S. *Nat. Mater.* **2003**, *2*, 827.
(2) Kiran, B.; Bulusu, S.; Zhai, H.-J.; Yoo, S.; Zeng, X. C.; Wang, L.-S. *Proc. Natl. Acad. Sci. U.S.A.* **2005**, *102*, 961.
(3) Chacko, S.; Kanhere, D. G.; Boustani, I. *Phys. Rev. B* **2003**, *68*, 035414.
(4) Boustani, I.; Rubio, A.; Alonso, J. *Chem. Phys. Lett.* **1999**, *311*, 21.
(5) Quandt, A.; Boustani, I. *ChemPhysChem* **2005**, *6*, 2001.
(6) Boustani, I.; Quandt, A. *Europhys. Lett.* **1997**, *39*, 527.
(7) Ciuparu, D.; Klie, R. F.; Zhu, Y.; Pfefferle, L. *J. Phys. Chem. B* **2004**, *108*, 3967.
(8) Lau, K. C.; Pati, R.; Pandey, R.; Pineda, A. C. *Chem. Phys. Lett.* **2006**, *418*, 549.
(9) Cabria, I.; Lopez, M. J.; Alonso, J. A. *Nanotechnology* **2006**, *17*, 778.
(10) Xu, T. T.; Zheng, J.-G.; Wu, N.; Nicholls, A. W.; Roth, J. R.; Dikin, D. A.; Ruoff, R. S. *Nano Lett.* **2004**, *4*, 963.
(11) Kunstmann, J.; Quandt, A. *Phys. Rev. B* **2006**, *74*, 035413.
(12) Szwacki, N. G.; Sadrzadeh, A.; Yakobson, B. I. *Phys. Rev. Lett.* **2007**, *98*, 166804.
(13) Tang, H.; Ismail-Beigi, S. *Phys. Rev. Lett.* **2007**, *99*, 115501.
(14) Miller, J. *Phys. Today* **2007**, *60*, 20.
(15) Lau, K. C.; Pandey, R. *J. Phys. Chem. C* **2007**, *111*, 2906.
(16) Dresselhaus, M. S.; Dresselhaus, G.; Eklund, P. C. *Science of Fullerenes and Carbon Nanotubes*; Academic Press: London, 1996.
(17) Yakobson, B. I.; Smalley, R. E. *Am. Sci.* **1997**, *85*, 324.
(18) Tans, S. J.; Devoret, M. H.; Dai, H. J.; Thess, A.; Smalley, R. E.; Geerligs, L. J.; Dekker, C. *Nature (London)* **1997**, *386*, 474.
(19) Kudin, K. N.; Scuseria, G. E.; Yakobson, B. I. *Phys. Rev. B* **2001**, *64*, 235406.
(20) Hernandez, E.; Goze, C.; Bernier, P.; Rubio, A. *Phys. Rev. Lett.* **1998**, *80*, 4502.
(21) Sanchez-Portal, D.; Artacho, E.; Soler, J. M.; Rubio, A.; Ordejon, P. *Phys. Rev. B* **1999**, *59*, 12678.
(22) Yakobson, B. I.; Avouris, P. *Top. Appl. Phys.* **2001**, *80*, 287.
(23) Terrones, M.; Romo-Herrera, J. M.; Cruz-Silva, E.; Lopez-Uras, F.; Muoz-Sandoval, E.; Velazquez-Salazar, J. J.; Terrones, H.; Bando, Y.; Golberg, D. *Mater. Today* **2007**, *10*, 30.
(24) Loiseau, A.; Willaime, F.; Demoncy, N.; Hug, G.; Pascard, H. *Phys. Rev. Lett.* **1996**, *76*, 4737.
(25) Perdew, J. P.; Burke, K.; Ernzerhof, M. *Phys. Rev. Lett.* **1996**, *77*, 3865.
(26) Kresse, G.; Furthmüller, J. *Comput. Mater. Sci.* **1996**, *6*, 15.
(27) Kresse, G.; Hafner, J. *Phys. Rev. B* **1993**, *47*, 558.
(28) Kresse, G.; Joubert, D. *Phys. Rev. B* **1999**, *59*, 1758.
(29) Blöchl, P. E. *Phys. Rev. B* **1994**, *50*, 17953.
(30) Landau, L. D.; Lifshitz, E. M. *Elasticity Theory*; Pergamon: New York, 1986.
(31) Yakobson, B. I.; Couchman, L. S. *J. Nanopart. Res.* **2006**, *8*, 105.
(32) Reich, S.; Thomsen, C.; Maultzsch, J. *Carbon Nanotubes*; Wiley: Berlin, 2004.
(33) Szwacki, N. G.; Sadrzadeh, A.; Yakobson, B. I. *Phys. Rev. Lett.* **2008**, in press.
(34) Yang, X.; Ding, Y.; Ni, J. *Phys. Rev. B* **2008**, *77*, 041402.

NL073295O